

# Extension of continuum mechanics to the nanoscale

John C. Slattery\*, Eun-Suok Oh, Kaibin Fu

Department of Aerospace Engineering, Texas A&M University, 3141 TAMU, College Station, TX 77843-3141, USA

Received 19 December 2003; received in revised form 25 June 2004; accepted 30 June 2004

## Abstract

This is an extension of continuum mechanics to the nanoscale (not the molecular scale). In the context of continuum mechanics, nanoscale problems always involve the immediate neighborhood of a phase interface or the immediate neighborhood of a three-phase line of contact or common line. While the presentation is new, it is based upon a long history of important developments beginning with that of Hamaker (*Physica* 4 (1937) 1058).

We test this theory by using it to predict both the surface tensions of the *n*-alkanes and the static contact angles for the *n*-alkanes on PTFE and for several liquids on polydimethylsiloxane. In the case of surface tension and like the best previous theory, one adjustable parameter is required. For the contact angle predictions, no adjustable parameters are used. In both cases, the results are compared with previously published experimental data.

The results for the contact angle analysis also provide a successful test of a previously derived form of Young's equation for the true, rather than apparent, common line.

© 2004 Elsevier Ltd. All rights reserved.

**Keywords:** Films; Interface; Momentum transfer; Nanostructure; Contact angle; Disjoining pressure; Surface tension; Young's equation

## 1. Introduction

By *nanoscale* we mean the immediate neighborhood of a phase interface, where the behavior of each phase is altered by the intermolecular forces from the adjoining phase. We are generally talking about more than the effect of interfacial tension or energy, which is a correction for long-range intermolecular forces between two “semi-infinite” phases. But we are not talking about the interaction between molecules within a single phase. We assume that such molecular-scale interactions are taken into account with an appropriate bulk description for material behavior.

In the immediate neighborhood of a phase interface, material behavior differs from that observed at some distance from the interface. All (local) descriptions of material behavior at some distance from the interface are based upon the assumption that the material extends to “infinity”

(perhaps 100 nm) in all directions. Material points outside the immediate neighborhood of the interface are subjected to intermolecular forces only from one phase. Material points within the immediate neighborhood of a phase interface are subjected to intermolecular forces from both phases.

There is a large literature describing intermolecular forces and how they should be represented, and it is not our intention to review it here. We suggest as starting points for understanding this subject in more detail referring the books by Israelachvili (1991) and by Hirschfelder et al. (1954). But it will be helpful to note that the Lennard–Jones (6)–(12) potential is commonly recommended for non-polar dilute gases (Hirschfelder et al., 1954, p. 22)

$$\phi^{(A,B)} = 4\varepsilon^{(A,B)} \left[ \left( \frac{\sigma^{(A,B)}}{r} \right)^{12} - \left( \frac{\sigma^{(A,B)}}{r} \right)^6 \right]. \quad (1)$$

Here  $\phi^{(A,B)}$  is the potential energy for two molecules *A* and *B* separated by a distance *r*; the parameters  $\sigma^{(A,B)}$ ,  $\varepsilon^{(A,B)}$  represent the collision diameter and well depth.

\* Corresponding author. Tel.: +1-979-845-0407; fax: +1-979-845-6051.  
E-mail address: slattery@tamu.edu (J.C. Slattery).

The  $r^{-6}$  term describes attractive forces: the dispersion forces (London forces or induced-dipole-induced dipole forces) (Israelachvili, 1991, p. 83). The  $r^{-12}$  contribution represents short-range repulsive forces. The only caution necessary to observe here is that  $\phi^{(A,B)}$  cannot be allowed to become infinite;  $r$  cannot be allowed to go to zero; it can be no smaller than the sum of the effective radii of molecules of  $A$  and  $B$  or the effective distance between molecules of  $A$  and  $B$ .

Israelachvili (1991, pp. 113, 176) argues that, due to a fortuitous cancellation of errors, the  $r^{-12}$  repulsive potential can be successfully replaced by a hard-sphere repulsive potential, reducing Eq. (1) for  $r > \sigma$  to

$$\begin{aligned}\phi^{(A,B)} &= -\frac{C^{(AB)}}{r^6} \quad \text{for } r > \sigma^{(A,B)}, \\ &= \infty \quad \text{for } r \leq \sigma^{(A,B)}.\end{aligned}\quad (2)$$

There is also a large literature in which the effects of intermolecular forces are discussed at the continuum scale.

Hamaker (1937) adopted Eq. (2) in discussing the force between macroscopic bodies of condensed matter, writing (Israelachvili, 1991, p. 176)

$$C^{(AB)} = \frac{A^{(AB)}}{\pi^2 n^{(A)} n^{(B)}} \quad (3)$$

where  $A^{(AB)}$  is the Hamaker constant,  $n^{(A)}$  and  $n^{(B)}$  are the number densities at the concerned points in phases  $A$  and  $B$ . There are at least three drawbacks to the Hamaker relation that should be noted. First, in calculating the force between two macroscopic bodies, he assumed that the intermolecular forces could be added pairwise. Second,  $A^{(AB)}$  is assumed to be geometry independent. Third, with increasing  $r$ , the attractive force decays even faster than  $r^{-6}$ , approaching  $r^{-7}$ . This is referred to as the *retardation* effect (Casimir and Polder, 1948).

To avoid these limitations, Lifshitz (1956) developed what we now refer to as *Lifshitz theory* by describing the multi-body interaction in the fluctuating electromagnetic field created by the material. Dzyaloshinskii et al. (1961) generalized Lifshitz theory, using quantum field theory. The results have the same form as those obtained using pairwise additivity as suggested by Hamaker (1937), but the value of the effective Hamaker constant is dependent on a number of effects. Mahanty and Ninham (1976) discussed the dependence of the effective Hamaker constant upon the macroscopic geometry. Hough and White (1980) employed Lifshitz theory to calculate non-retarded Hamaker constants. Russel et al. (1989) gave an expression for the effective Hamaker constant that includes the effects of retardation and properly reduces to the results of Hough and White (1980) when the effects of retardation are absent. Bowen and Jenner (1995) have examined all of these issues, and they recommend a calculation for an effective, Lifshitz type, Hamaker constant that is both screened and retarded and that is geometry independent.

In what follows, we propose to incorporate the effect of intermolecular forces from adjacent phases as a body force in the standard developments of continuum mechanics. Following the developments described above, we can completely avoid the difficulties of pairwise additivity by employing effective, Lifshitz-type, Hamaker constants (Israelachvili, 1991, p. 180; Bowen and Jenner, 1995).

In particular, using Eqs. (2) and (3), we will express the potential energy per unit volume of  $A$  per unit volume of  $B$  as

$$\begin{aligned}n^{(A)} n^{(B)} \phi^{(ACB)} &= -\frac{C^{(AB)} n^{(A)} n^{(B)}}{r^6} \\ &= -\frac{A^{(ACB)}}{\pi^2 r^6}.\end{aligned}\quad (4)$$

Here  $A^{(ACB)}$  denotes the effective, Lifshitz-type, Hamaker constant for species  $A$  and  $B$  interacting across an intermediate phase  $C$ . If there is no intermediate phase or the intermediate phase is a vacuum, we will use the notation  $A^{(AB)}$ . The corresponding force  $\mathbf{f}^{(A,B)}(\mathbf{r}^{(A)}, \mathbf{r}^{(B)})$  per unit volume of phase  $A$  per unit volume of phase  $B$  at a point  $\mathbf{r}^{(A)}$  in phase  $A$  attributable to the material at point  $\mathbf{r}^{(B)}$  in phase  $B$  is

$$\begin{aligned}\mathbf{f}^{(A,B)} &= -\nabla \left( n^{(A)} n^{(B)} \phi^{(A,B)} \right) \\ &= \nabla \left( \frac{A^{(ACB)}}{\pi^2 r^6} \right).\end{aligned}\quad (5)$$

As explained above, because we propose to use an effective, Lifshitz type, Hamaker constant  $A^{(ACB)}$  such as that recommended by Bowen and Jenner (1995), we will assume that these two-point forces are pairwise additive and therefore that they can be integrated.

## 2. The correction

Our premise is that material behavior within the interfacial region can be represented as bulk material behavior corrected for the intermolecular forces from the adjoining phase. In particular, we recognize the equivalence of stresses and body forces (Truesdell and Toupin, 1960, p. 549).

There are four descriptions of the interfacial region, each view having its own somewhat different notation.

- Ideally, we would wish to use the true descriptions of material behavior appropriate everywhere, including the interfacial region. Using these descriptions, we would refer to  $\mathbf{v}^{(I)}$ ,  $\mathbf{T}^{(I)}$  and  $\rho^{(I)}$  as the velocity, stress tensor and density. No excess quantities would be associated with any dividing surface. The problem with this view is that in general we will not know the appropriate descriptions of behavior in the interfacial regions.
- In the second view, we use everywhere the descriptions of material behavior appropriate outside the interfacial region (bulk material behavior). The effects of the

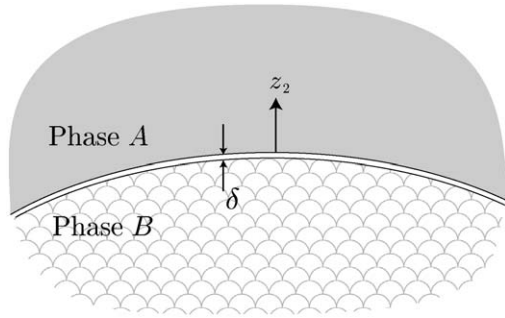


Fig. 1. A material body consisting of two adjoining phases, A and B.

interfacial region are taken into account by the excess quantities assigned to the corresponding dividing surface (Slattery, 1990, Sections 1.3.5 and 2.1.6). By  $\mathbf{v}^{(\sigma)}$ ,  $\mathbf{T}^{(\sigma)}$  and  $\rho^{(\sigma)}$ , we mean the corresponding surface velocity, surface stress tensor, and surface mass density.

- (c) In the third view described in Fig. 1, we again use the descriptions of material behavior appropriate outside the interfacial region (bulk material behavior), but no excess properties are assigned to the dividing surface. By  $\mathbf{v}^{(I,\text{bulk})}$ ,  $\mathbf{T}^{(I,\text{bulk})}$  and  $\rho^{(I,\text{bulk})}$ , we indicate the velocity, stress tensor and density determined using the bulk descriptions of material behavior, corrected for intermolecular forces from the adjoining phase as described below. The two phases are separated by a distance  $\delta$ , which physically corresponds to the sum of the effective radii of the A and B molecules or the effective distance between molecules of A and B.<sup>1</sup> These surfaces should not be thought of as dividing surfaces, since there are no excess properties associated with them. If a dividing surface is introduced, it will be located in a standard manner (Slattery, 1990, Sections 1.3.6 and 5.2.3). The differential and jump mass balances follow by analogy take standard forms (Slattery, 1990, Sections 1.3.5 and 5.4.1):

$$\frac{d_{(m)}\rho^{(I,\text{bulk})}}{dt} + \rho^{(I,\text{bulk})} \text{div } \mathbf{v}^{(I,\text{bulk})} = 0, \quad (6)$$

$$\left[ \rho^{(I,\text{bulk})} (\mathbf{v}^{(I,\text{bulk})} - \mathbf{v}^{(\sigma)}) \cdot \boldsymbol{\xi} \right] = 0. \quad (7)$$

We note that the jump is now over both singular surfaces in Fig. 1. The boldface brackets denote the jump of the quantity enclosed across the interface between phases A and B:

$$\left[ \mathbf{s}\boldsymbol{\xi} \right] \equiv \mathbf{s}^{(A)} \boldsymbol{\xi}^{(A)} + \mathbf{s}^{(B)} \boldsymbol{\xi}^{(B)}, \quad (8)$$

<sup>1</sup> Fu et al. (2004), working in the context of supercritical adsorption on Graphon and representing  $\phi^{(AA)}$  and  $\phi^{(AB)}$ , determines  $\delta^{(AB)}$  by requiring  $\Phi^{(A)} = 0$ . We believe that this can be done only with the Lennard–Jones potential which accounts for both repulsive and attractive forces.

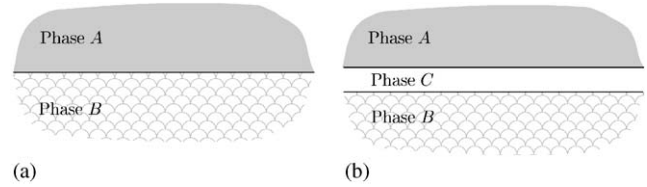


Fig. 2. For simplicity, the dividing surfaces and the two singular surfaces for each interface are shown as a single curve. Two cases are illustrated: (a) two semi-infinite phases A and B and (b) two semi-infinite phases A and B separated by a thin film of phase C.

where  $\boldsymbol{\xi}^{(\alpha)}$  is the unit normal to the interface pointing into phase  $\alpha$ . In the same way, we can write the differential and jump momentum balances in almost the standard forms (Slattery, 1990, Sections 5.4.1 and 5.4.2):

$$\rho^{(I,\text{bulk})} \frac{d_{(m)}\mathbf{v}^{(I,\text{bulk})}}{dt} = \text{div } \mathbf{T}^{(I,\text{bulk})} + \rho^{(I,\text{bulk})} \mathbf{b} + \mathbf{b}^{(\text{corr})}, \quad (9)$$

$$\left[ \rho^{(I,\text{bulk})} (\mathbf{v}^{(I,\text{bulk})} \cdot \boldsymbol{\xi} - v_{(\boldsymbol{\xi})}^{(\sigma)})^2 \boldsymbol{\xi} - \mathbf{T}^{(I,\text{bulk})} \cdot \boldsymbol{\xi} \right] = 0. \quad (10)$$

Here  $\mathbf{b}$  is the body force per unit mass, typically gravity;  $\mathbf{b}^{(\text{corr})}$  is a body force per unit volume introduced to correct for the use of bulk material behavior in the interfacial region.

- (d) The fourth view is a variation on view (b) above, and it is used only in the case of a thin film. The only difference is that we add a body force  $\mathbf{b}^{(\text{corr})\infty}$  that corrects for overlapping intermolecular forces. The excess properties in (b) are those attributable to a single, isolated interface. In the case of a thin film, the two interfaces are not isolated, and each phase is subjected to long-range intermolecular forces from the other two.

In order to illustrate the estimation of  $\mathbf{b}^{(\text{corr})}$ , consider the two cases shown in Fig. 2.

- (1) For the two phases shown in Fig. 2(a), in estimating  $\mathbf{b}^{(A,\text{corr})}$  we will
- subtract the force per unit volume at a point in phase A attributable to that portion of phase A that has been replaced by phase B, and
  - add the force per unit volume at this same point in phase A attributable to phase B.
- In reality, the effective replacement region  $R^{(B)}$  may be no more than 100 nm thick, since outside this region the intermolecular forces between phases A and B go to zero.
- (2) Let us now consider the thin film as shown in Fig. 2(b). In order to estimate  $\mathbf{b}^{(A,\text{corr})}$ , we will
- subtract the force per unit volume at a point in phase A attributable to that portion of phase A that has been replaced by phases C and B,
  - add force per unit volume at this same point in phase A attributable to phase C, and

- add force per unit volume at this point in phase A attributable to phase B.

### 3. One dividing surface

Consider two semi-infinite phases *A* and *B* shown in Fig. 2(a), although it will not be necessary to make any assumption about the configuration of the interface. In particular, it is not necessary to assume that the dividing surface is a plane. As suggested in the assumptions above, the net correction for intermolecular forces  $\mathbf{b}^{(A,\text{corr})}$  at each point in phase *A* within the immediate neighborhood of the dividing surface is

$$\begin{aligned} \mathbf{b}^{(A,\text{corr})} &\equiv - \int_{R^{(B)}} \mathbf{f}^{(A,A)} \, d\mathbf{r} + \int_{R^{(B)}} \mathbf{f}^{(A,B)} \, d\mathbf{r} \\ &= \int_{R^{(B)}} \nabla(n^{(A)})^2 \phi^{(A,A)} \, d\mathbf{r} \\ &\quad - \int_{R^{(B)}} \nabla(n^{(A)}n^{(B)}) \phi^{(A,B)} \, d\mathbf{r} \\ &= -\nabla\Phi^{(A,\text{corr})}, \end{aligned} \quad (11)$$

where

$$\begin{aligned} \Phi^{(A,\text{corr})} &\equiv - \int_{R^{(B)}} n^{(A)2} \phi^{(A,A)} \, d\mathbf{r} \\ &\quad + \int_{R^{(B)}} n^{(A)}n^{(B)} \phi^{(A,B)} \, d\mathbf{r}. \end{aligned} \quad (12)$$

In a similar manner,

$$\begin{aligned} \mathbf{b}^{(B,\text{corr})} &\equiv - \int_{R^{(A)}} \mathbf{f}^{(B,B)} \, d\mathbf{r} + \int_{R^{(A)}} \mathbf{f}^{(A,B)} \, d\mathbf{r} \\ &= \int_{R^{(A)}} \nabla(n^{(B)})^2 \phi^{(B,B)} \, d\mathbf{r} \\ &\quad - \int_{R^{(A)}} \nabla(n^{(A)}n^{(B)}) \phi^{(A,B)} \, d\mathbf{r} \\ &= -\nabla\Phi^{(B,\text{corr})} \end{aligned} \quad (13)$$

in which

$$\begin{aligned} \Phi^{(B,\text{corr})} &\equiv - \int_{R^{(A)}} n^{(B)2} \phi^{(B,B)} \, d\mathbf{r} \\ &\quad + \int_{R^{(A)}} n^{(A)}n^{(B)} \phi^{(A,B)} \, d\mathbf{r}. \end{aligned} \quad (14)$$

Fu et al. (2004) employed Eqs. (11), (12), and the differential momentum balance to discuss supercritical adsorption or local densification of a supercritical gas on an impermeable graphon. Following Steele (1973, 1974, 1978), they used the Lennard–Jones potential with standard parameters for  $\phi^{(AA)}$  (Bird et al., 2002, p. 804) and for  $\phi^{(AB)}$  (Steele, 1974, p. 56). Using no adjustable parameters, they presented favorable comparisons with experimental data and alternative theories from several groups.

#### 3.1. One dividing surface: with interfacial energy or tension

Let us now adopt view (b) of the interfacial region, in which bulk descriptions of material behavior are used, but excess properties are assigned to the dividing surface. It is not necessary to make any assumption about the configuration of the dividing surface, but for the sake of simplifying the argument, we will neglect the effects of any external force such as gravity.

It has been shown that (Slattery, 1990, p. 164)

$$\begin{aligned} \mathbf{T}^{(\sigma)} &\equiv \left\{ \int_0^{\lambda^+} (\mathbf{T}^{(I)} - \mathbf{T}) \, d\lambda \right\} \cdot \mathbf{P} \\ &\quad + \left\{ \int_{\lambda^-}^{-\delta} (\mathbf{T}^{(I)} - \mathbf{T}) \, d\lambda \right\} \cdot \mathbf{P}, \end{aligned} \quad (15)$$

where  $\mathbf{P}$  is the projection tensor (Slattery, 1990, p. 1085),  $\lambda$  is the distance measured along the normal to the dividing surface, and  $\delta$  is the distance separating the two phases.

Let us use the results above to compute  $\mathbf{T}^{(\sigma)}$ .

We will approximate (since we have no way of knowing the true description of behavior in the interfacial region)

$$\mathbf{T}^{(I)} \doteq \mathbf{T}^{(I,\text{bulk})}. \quad (16)$$

In view of Eq. (5), Eq. (9) reduces to

$$\begin{aligned} \rho^{(I,\text{bulk})} \frac{d_{(m)} \mathbf{v}^{(I,\text{bulk})}}{dt} &= \text{div} (\mathbf{T}^{(I,\text{bulk})} - \Phi^{(\text{corr})} \mathbf{I}) \\ &\quad + \rho^{(I,\text{bulk})} \mathbf{b}. \end{aligned} \quad (17)$$

Comparing this with the usual form of the differential momentum balance (Slattery, 1999, p. 34), we can identify

$$\mathbf{T} = \mathbf{T}^{(I,\text{bulk})} - \Phi^{(\text{corr})} \mathbf{I}. \quad (18)$$

Given Eqs. (16) and (18), Eq. (15) reduces to

$$\begin{aligned} \mathbf{T}^{(\sigma)} &= \left\{ \int_0^{\lambda^+} \Phi^{(A,\text{corr})} \mathbf{I} \, d\lambda + \int_{\lambda^-}^{-\delta^{(AB)}} \Phi^{(B,\text{corr})} \mathbf{I} \, d\lambda \right\} \cdot \mathbf{P} \\ &= \int_0^{\lambda^+} \Phi^{(A,\text{corr})} \, d\lambda \, \mathbf{P} + \int_{\lambda^-}^{-\delta^{(AB)}} \Phi^{(B,\text{corr})} \, d\lambda \, \mathbf{P} \end{aligned} \quad (19)$$

or

$$\mathbf{T}^{(\sigma)} = \gamma \mathbf{P}, \quad (20)$$

where

$$\begin{aligned} \gamma &\equiv \int_0^{\lambda^+} \Phi^{(A,\text{corr})} \, d\lambda + \int_{\lambda^-}^{-\delta^{(AB)}} \Phi^{(B,\text{corr})} \, d\lambda \\ &= \int_0^{\infty} \Phi^{(A,\text{corr})} \, d\lambda + \int_{-\infty}^{-\delta^{(AB)}} \Phi^{(B,\text{corr})} \, d\lambda \end{aligned} \quad (21)$$

is interfacial tension or interfacial energy.

It is important to realize that  $\gamma$  represents the correction of intermolecular forces in the immediate neighborhood of a single dividing surface. But Eq. (20) also tells us that

we should not expect to see surface viscous effects with clean interfaces such as we are considering in these first four chapters, which is in agreement with common observations.

Just to emphasize the point, since we are employing interfacial energy or tension, the stresses that appear in the jump momentum balance are the bulk stresses rather than the interfacial stresses.

### 3.1.1. Assuming Eqs. (2) and (3)

Starting with Eqs. (2) and (3), we can compute from Eqs. (12) and (14)

$$\Phi^{(A,\text{corr})} = \frac{A^{(AA)}}{6\pi(\delta^{(AA)} + z_2)^3} - \frac{A^{(AB)}}{6\pi(\delta^{(AB)} + z_2)^3} \quad (22)$$

and

$$\Phi^{(B,\text{corr})} = \frac{A^{(AB)}}{6\pi z_2^3} - \frac{A^{(BB)}}{6\pi(\delta^{(AB)} - \delta^{(BB)} + z_2)^3}, \quad (23)$$

where  $\delta^{(\alpha\beta)}$  is the effective distance between molecules of  $\alpha$  and  $\beta$ . Following Fu et al. (2004), we will require

$$\text{at } z_2 = 0 : \quad \Phi^{(A,\text{corr})} = 0 \quad (24)$$

or

$$\frac{A^{(AA)}}{\delta^{(AA)^3} = \frac{A^{(AB)}}{\delta^{(AB)^3}} \quad (25)$$

and

$$\text{at } z_2 = -\delta^{(AB)} : \quad \Phi^{(B,\text{corr})} = 0 \quad (26)$$

or

$$\frac{A^{(AB)}}{\delta^{(AB)^3} = \frac{A^{(BB)}}{\delta^{(BB)^3}}. \quad (27)$$

These together with Eq. (21) give us

$$\begin{aligned} \gamma &= \frac{A^{(AA)}}{12\pi\delta^{(AA)^2} - \frac{A^{(AB)}}{6\pi\delta^{(AB)^2} + \frac{A^{(BB)}}{12\pi\delta^{(BB)^2}} \\ &= \frac{\delta^{(AA)}}{12\pi} \frac{A^{(BB)}}{\delta^{(BB)^3} - \frac{\delta^{(AB)}}{6\pi} \frac{A^{(BB)}}{\delta^{(BB)^3} + \frac{A^{(BB)}}{12\pi\delta^{(BB)^3}} \\ &= \left( \frac{\delta^{(AA)}}{\delta^{(BB)}} - 2 \frac{\delta^{(AB)}}{\delta^{(BB)}} + 1 \right) \frac{A^{(BB)}}{12\pi\delta^{(BB)^3}} \\ &= \left[ \left( \frac{A^{(AA)}}{A^{(BB)}} \right)^{1/3} - 2 \left( \frac{A^{(AB)}}{A^{(BB)}} \right)^{1/3} + 1 \right] \frac{A^{(BB)}}{12\pi\delta^{(BB)^3}}. \quad (28) \end{aligned}$$

Note that Eq. (28) should not be expected to represent very well the surface or interfacial tensions for liquids with strong hydrogen bonding; our simple representation of point-to-

point forces (2) only attempts to take into account dispersion or van der Waals forces (Israelachvili, 1991, p. 204).

If we assume that phase A is a gas, we can neglect  $A^{(AA)}$  and  $A^{(AB)}$  with respect to  $A^{(BB)}$  and Eq. (33) reduces to<sup>2</sup>

$$\gamma = \frac{A^{(BB)}}{24\pi\delta^{(BB)^2}} \quad (29)$$

using a much different argument, in which a body was ruptured by tensile forces to form two pieces and two interfaces. Deformation of the body prior to rupture was not taken into account. In order to fit experimental data for a variety of system, he recommended  $\delta^{(BB)} = 0.165$  nm. In the context of Eq. (33), we would say

$$\begin{aligned} \delta^{(BB)} &= 0.165 \times \sqrt{2} \\ &= 0.233 \text{ nm}. \quad (30) \end{aligned}$$

Israelachvili (1973) suggests that, within phase A,  $\delta^{(AA)}$  be viewed as the mean distance between the centers of individual molecules, units of molecules, or atoms and that it be estimated as

$$\delta^{(AA)} = 0.916[M^{(A)}/(\rho^{(A)}n_aN)]^{1/3}. \quad (31)$$

Here  $M^{(A)}$  is the molecular weight of phase A,  $n_a$  is the number of atoms per molecule,  $N$  is Avogadro's constant ( $6.023 \times 10^{23} \text{ mol}^{-1}$ ), and  $\rho^{(A)}$  the mass density of phase A. In arriving at Eq. (31), the atoms have been assumed to be in a close packing arrangement.

For a molecule consisting of a repeating unit, such as an  $n$ -alkane with  $-\text{CH}_2-$  being the repeating unit, we suggest a simple picture in which the molecules are arranged in such a manner that the *repeating units* are in a close packing arrangement. Retracing the argument of Israelachvili (1973), we have instead

$$\delta^{(AA)} = 0.916[M^{(A)}/(\rho^{(A)}n_uN)]^{1/3}, \quad (32)$$

where  $n_u$  is the number of repeating units in the molecule. This last is similar to the suggestion of Padday and Uffindell (1968), who replaced  $M/n_u$  by the  $-\text{CH}_2-$  group weight and took the coefficient to be unity.

$$\gamma = \frac{A^{(BB)}}{12\pi\delta^{(BB)^2}}. \quad (33)$$

In preparing Table 1 to test the validity of Eq. (33), we have used  $\delta^{(BB)} = 0.79 \times$  Eq. (32), a one-parameter fit of the experimental data similar to Eq. (30), essentially the one-parameter fit of experimental data recommended by

<sup>2</sup> Israelachvili (1991, pp. 202, 203, 313) arrived at a similar expression.

Table 1  
Comparisons of calculated and measured values of surface tensions for *n*-alkanes

<i>n</i>	$A^{(BB)a}$ ( $10^{-20}$ J)	$\delta^{(BB)b}$ (nm)	$\delta^{(BB)c}$ (nm)	$\gamma_{\text{meas.}}^d$ ( $\text{mJ m}^{-2}$ )	$\gamma_{\text{calc.}}^e$ ( $\text{mJ m}^{-2}$ )	$\gamma_{\text{calc.}}^f$ ( $\text{mJ m}^{-2}$ )
5	3.74	0.205	0.309	16.0	18.2	16.6
6	4.06	0.203	0.303	18.4	19.8	18.8
7	4.31	0.201	0.299	20.3	21.0	20.5
8	4.49	0.200	0.296	21.8	21.9	21.8
9	4.66	0.199	0.294	22.9	22.7	22.9
10	4.81	0.198	0.292	23.9	23.4	23.9
11	4.87	0.198	0.291	24.7	23.7	24.4
12	5.03	0.197	0.289	25.4	24.5	25.6
14	5.09	0.196	0.287	26.7	24.8	26.2
16	5.22	0.196	0.286	27.6	25.4	27.1

<sup>a</sup>Calculated by Hough and White (1980).

<sup>b</sup>Calculated using Eq. (31).

<sup>c</sup>Calculated using Eq. (32).

<sup>d</sup>Measured by Jasper and Kring (1955).

<sup>e</sup>Calculated by Israelachvili (1991) using Eqs. (30) and (33).

<sup>f</sup>Calculated using Eq. (33) and  $\delta^{(BB)} = 0.79 \times \text{Eq. (32)}$ .

Israelachvili (1991, pp. 202, 203, 313). For broader variety of systems, Israelachvili (1991, p. 204) presents an interesting comparison of Eq. (29) using  $\delta^{(BB)} = 0.165$  nm, which is equivalent to Eq. (33) with Eq. (30).

#### 4. One thin film

Consider now the thin film shown in Fig. 2(b). It is not necessary that the dividing surfaces be planes or equidistant surfaces.

As suggested in the assumptions above, the net correction for intermolecular forces at each point in phase A is

$$\begin{aligned}
 \mathbf{b}^{(A,\text{corr})} &\equiv - \int_{R^{(B+C)}} \mathbf{f}^{(A,A)} \, d\mathbf{r} + \int_{R^{(C)}} \mathbf{f}^{(A,C)} \, d\mathbf{r} \\
 &\quad + \int_{R^{(B)}} \mathbf{f}^{(A,B)} \, d\mathbf{r} \\
 &= \nabla \int_{R^{(B+C)}} n^{(A)2} \phi^{(A,A)} \, d\mathbf{r} \\
 &\quad - \nabla \int_{R^{(C)}} n^{(A)} n^{(C)} \phi^{(A,C)} \, d\mathbf{r} \\
 &\quad - \nabla \int_{R^{(B)}} n^{(A)} n^{(B)} \phi^{(A,B)} \, d\mathbf{r} \\
 &= - \nabla \Phi^{(A,\text{corr})}, \tag{34}
 \end{aligned}$$

where

$$\begin{aligned}
 \Phi^{(A,\text{corr})} &\equiv - \int_{R^{(B+C)}} n^{(A)2} \phi^{(A,A)} \, d\mathbf{r} \\
 &\quad + \int_{R^{(C)}} n^{(A)} n^{(C)} \phi^{(A,C)} \, d\mathbf{r} \\
 &\quad + \int_{R^{(B)}} n^{(A)} n^{(B)} \phi^{(A,B)} \, d\mathbf{r}. \tag{35}
 \end{aligned}$$

In a similar way, we conclude that

$$\begin{aligned}
 \mathbf{b}^{(B,\text{corr})} &\equiv - \int_{R^{(A+C)}} \mathbf{f}^{(B,B)} \, d\mathbf{r} + \int_{R^{(C)}} \mathbf{f}^{(B,C)} \, d\mathbf{r} \\
 &\quad + \int_{R^{(A)}} \mathbf{f}^{(A,B)} \, d\mathbf{r} \\
 &= \nabla \int_{R^{(A+C)}} n^{(B)2} \phi^{(B,B)} \, d\mathbf{r} \\
 &\quad - \nabla \int_{R^{(C)}} n^{(B)} n^{(C)} \phi^{(B,C)} \, d\mathbf{r} \\
 &\quad - \nabla \int_{R^{(A)}} n^{(A)} n^{(B)} \phi^{(A,B)} \, d\mathbf{r} \\
 &= - \nabla \Phi^{(B,\text{corr})}, \tag{36}
 \end{aligned}$$

$$\begin{aligned}
 \mathbf{b}^{(C,\text{corr})} &\equiv - \int_{R^{(A+B)}} \mathbf{f}^{(C,C)} \, d\mathbf{r} + \int_{R^{(A)}} \mathbf{f}^{(A,C)} \, d\mathbf{r} \\
 &\quad + \int_{R^{(B)}} \mathbf{f}^{(B,C)} \, d\mathbf{r} \\
 &= \nabla \int_{R^{(A+B)}} n^{(C)2} \phi^{(C,C)} \, d\mathbf{r} \\
 &\quad - \nabla \int_{R^{(A)}} n^{(A)} n^{(C)} \phi^{(A,C)} \, d\mathbf{r} \\
 &\quad - \nabla \int_{R^{(B)}} n^{(B)} n^{(C)} \phi^{(B,C)} \, d\mathbf{r} \\
 &= - \nabla \Phi^{(C,\text{corr})}. \tag{37}
 \end{aligned}$$

Here

$$\begin{aligned}
 \Phi^{(B,\text{corr})} &\equiv - \int_{R^{(A+C)}} n^{(B)2} \phi^{(B,B)} \, d\mathbf{r} \\
 &\quad + \int_{R^{(C)}} n^{(B)} n^{(C)} \phi^{(B,C)} \, d\mathbf{r} \\
 &\quad + \int_{R^{(A)}} n^{(A)} n^{(B)} \phi^{(A,B)} \, d\mathbf{r} \tag{38}
 \end{aligned}$$

and

$$\begin{aligned} \Phi^{(C,\text{corr})} &\equiv - \int_{R^{(A+B)}} n^{(C)2} \phi^{(C,C)} \, \mathbf{dr} \\ &+ \int_{R^{(A)}} n^{(A)} n^{(C)} \phi^{(A,C)} \, \mathbf{dr} \\ &+ \int_{R^{(B)}} n^{(B)} n^{(C)} \phi^{(B,C)} \, \mathbf{dr}. \end{aligned} \quad (39)$$

Note that these results also apply to a discontinuous film forming a common line as shown in Fig. 3.

#### 4.1. One thin film: with interfacial energy or tension in both interfaces

Let us now adopt view (d) of the interfacial region as outlined in the introduction to this section.

For the case considered in Section 4, let us specifically assume that phase A is a gas, phase B a liquid, and phase C a solid. We will now adopt view (b) of the interfacial region, in which interfacial energies or tensions are introduced in both dividing surface.

This means that, in contrast with the discussion in Section 3.1,  $\gamma^{(AC)}$  and  $\gamma^{(BC)}$  cannot fully account for the correction that must be made to the intermolecular forces. There is an additional correction to be made, which we will develop here. As an example, for phase A we will name this correction  $\mathbf{b}^{(A,\text{corr})\infty}$ , in order to distinguish it from  $\mathbf{b}^{(A,\text{corr})}$  developed above.

In particular, the correction for intermolecular forces at any point in phase A now becomes Eq. (34) minus Eqs. (11) and (13), both of which have to be suitably modified:

$$\begin{aligned} \mathbf{b}^{(A,\text{corr})\infty} &\equiv \mathbf{b}^{(A,\text{corr})} - \nabla \int_{R^{(B+C)}} n^{(A)2} \phi^{(A,A)} \, \mathbf{dr} \\ &+ \nabla \int_{R^{(B+C)}} n^{(A)} n^{(C)} \phi^{(A,C)} \, \mathbf{dr} \\ &- \nabla \int_{R^{(B)}} n^{(C)2} \phi^{(C,C)} \, \mathbf{dr} \\ &+ \nabla \int_{R^{(B)}} n^{(B)} n^{(C)} \phi^{(B,C)} \, \mathbf{dr} \\ &= \nabla \int_{R^{(B)}} [n^{(A)} n^{(C)} \phi^{(A,C)} - n^{(A)} n^{(B)} \phi^{(A,B)} \\ &\quad - n^{(C)2} \phi^{(C,C)} + n^{(B)} n^{(C)} \phi^{(B,C)}] \, \mathbf{dr} \\ &= - \nabla \Phi^{(A,\text{corr})\infty}, \end{aligned} \quad (40)$$

where

$$\begin{aligned} \Phi^{(A,\text{corr})\infty} &\equiv - \int_{R^{(B)}} [n^{(A)} n^{(C)} \phi^{(A,C)} - n^{(A)} n^{(B)} \phi^{(A,B)} \\ &\quad - n^{(C)2} \phi^{(C,C)} + n^{(B)} n^{(C)} \phi^{(B,C)}] \, \mathbf{dr}. \end{aligned} \quad (41)$$

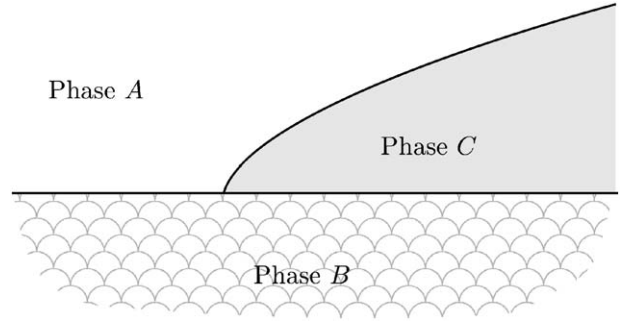


Fig. 3. A thin discontinuous film C forms a common line.

In a similar manner, we find

$$\begin{aligned} \mathbf{b}^{(B,\text{corr})\infty} &\equiv \mathbf{b}^{(B,\text{corr})} - \nabla \int_{R^{(A+C)}} n^{(B)2} \phi^{(B,B)} \, \mathbf{dr} \\ &+ \nabla \int_{R^{(A+C)}} n^{(B)} n^{(C)} \phi^{(B,C)} \, \mathbf{dr} \\ &+ \nabla \int_{R^{(A+C)}} n^{(B)} n^{(C)} \phi^{(B,C)} \, \mathbf{dr} \\ &- \nabla \int_{R^{(A)}} n^{(C)2} \phi^{(C,C)} \, \mathbf{dr} \\ &+ \nabla \int_{R^{(A)}} n^{(A)} n^{(C)} \phi^{(A,C)} \, \mathbf{dr} \\ &= \nabla \int_{R^{(A)}} [n^{(B)} n^{(C)} \phi^{(B,C)} - n^{(A)} n^{(B)} \phi^{(A,B)} \\ &\quad - n^{(C)2} \phi^{(C,C)} + n^{(A)} n^{(C)} \phi^{(A,C)}] \, \mathbf{dr} \\ &= - \nabla \Phi^{(B,\text{corr})\infty} \end{aligned} \quad (42)$$

and

$$\begin{aligned} \mathbf{b}^{(C,\text{corr})\infty} &\equiv \mathbf{b}^{(C,\text{corr})} - \nabla \int_{R^{(A)}} n^{(C)2} \phi^{(C,C)} \, \mathbf{dr} \\ &+ \nabla \int_{R^{(A)}} n^{(A)} n^{(C)} \phi^{(A,C)} \, \mathbf{dr} \\ &- \nabla \int_{R^{(B)}} n^{(C)2} \phi^{(C,C)} \, \mathbf{dr} \\ &+ \nabla \int_{R^{(B)}} n^{(B)} n^{(C)} \phi^{(B,C)} \, \mathbf{dr} \\ &= - \nabla \Phi^{(C,\text{corr})\infty} \\ &= 0 \end{aligned} \quad (43)$$

in which

$$\begin{aligned} \Phi^{(B,\text{corr})\infty} &\equiv - \int_{R^{(A)}} [n^{(B)} n^{(C)} \phi^{(B,C)} - n^{(A)} n^{(B)} \phi^{(A,B)} \\ &\quad - n^{(C)2} \phi^{(C,C)} + n^{(A)} n^{(C)} \phi^{(A,C)}] \, \mathbf{dr} \end{aligned} \quad (44)$$

and

$$\Phi^{(C,\text{corr})\infty} = 0. \quad (45)$$

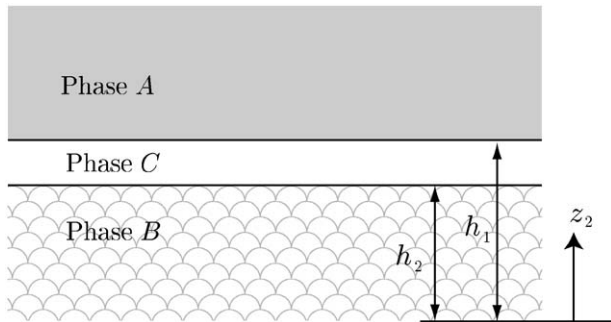


Fig. 4. A thin film bounded by two parallel, plane interfaces.

No assumption is made here about the configuration of the thin film  $C$ , and they are immediately applicable to the discontinuous film shown in Fig. 3 as explained in Section 4.2.

#### 4.1.1. Parallel plane interfaces

In order to illustrate the results derived here, consider a thin film of phase  $C$  bounded by parallel, plane interfaces in which interfacial tensions or energies have been introduced. The film is unbounded in  $z_1$  and  $z_3$  directions; its thickness is the difference between  $h_1$  and  $h_2$  as illustrated in Fig. 4. Using Eqs. (41) and (44), we can show in region  $A$

$$\Phi^{(A, \text{corr})\infty} = -\frac{A^{(ACB)} - A^{(AC)} + A^{(CC)} - A^{(BC)}}{6\pi(z_2 - h_2)^3}$$

and in region  $B$

$$\Phi^{(B, \text{corr})\infty} = \frac{A^{(BC)} - A^{(ACB)} - A^{(CC)} + A^{(AC)}}{6\pi(h_1 - z_2)^3}.$$

For simplicity, let us neglect any effect of gravity within the interfacial region. It is common to introduce an extra stress

$$\mathbf{S} \equiv \mathbf{T} + P\mathbf{I} \quad (46)$$

and a modified pressure

$$\mathcal{P} \equiv P + \Phi^{(\text{corr})\infty}. \quad (47)$$

The physical significance of  $\mathcal{P}$  is that this is the thermodynamic pressure that would exist in the absence of the correction for intermolecular forces. This has the advantage that, if we are willing to assume  $\rho^{(I, \text{bulk})}$  is a constant within the interfacial region, the corrections for intermolecular forces drop out of the differential momentum balance (9)

$$\rho^{(I, \text{bulk})} \frac{d_{(m)} \mathbf{v}^{(I, \text{bulk})}}{dt} = -\nabla \mathcal{P} + \text{div} \mathbf{S}^{(I, \text{bulk})} \quad (48)$$

and appear only in the jump momentum balance (10)

$$\left[ \rho^{(I, \text{bulk})} \left( \mathbf{v}^{(I, \text{bulk})} \cdot \boldsymbol{\xi} - v_{(\boldsymbol{\xi})}^{(\sigma)} \right)^2 \boldsymbol{\xi} + \mathcal{P} \boldsymbol{\xi} - \Phi^{(\text{corr})\infty} \boldsymbol{\xi} - \mathbf{S}^{(I, \text{bulk})} \boldsymbol{\xi} \right] = 0. \quad (49)$$

Consider the interface between phases  $A$  and  $C$  in Fig. 4. Referring to Eqs. (45), (47) and (49), we see that

$$\begin{aligned} & \left[ \mathcal{P} \boldsymbol{\xi} - \Phi \boldsymbol{\xi} \right] \\ &= (\mathcal{P}^{(A)} - P^{(C)} - \Phi^{(A, \text{corr})\infty}) \boldsymbol{\xi}^{(A)} \\ &= \left( \mathcal{P}^{(A)} - P^{(C)} \right. \\ & \quad \left. - \frac{A^{(AC)} + A^{(BC)} - A^{(ACB)} - A^{(CC)}}{6\pi(h_1 - h_2)^3} \right) \boldsymbol{\xi}^{(A)}. \end{aligned} \quad (50)$$

Here  $\boldsymbol{\xi}^{(A)}$  is the unit normal to the interface pointing into phase  $A$ . In this context  $\Phi^{(A, \text{corr})\infty}$  may be referred to as the *disjoining pressure*, in the sense that it has the effect of changing  $P^{(C)}$ . A *positive disjoining pressure* or  $A^{(AC)} + A^{(BC)} > A^{(ACB)} + A^{(CC)}$  means that phases  $A$  and  $B$  would prefer to be in contact with phase  $C$  rather than each other, and the thickness of the film will tend to increase or *disjoin*. A *negative disjoining pressure* or  $A^{(AC)} + A^{(BC)} < A^{(ACB)} + A^{(CC)}$  means that phases  $A$  and  $B$  would prefer to be in contact with each other rather than phase  $C$ , and the thickness of the film will tend to decrease.

Here we have introduced the disjoining pressure only in the context of the correction for intermolecular forces. More generally, the disjoining pressure is introduced to describe both electrostatic forces and the correction for intermolecular forces. It is necessary only that the body force be representable in terms of a potential and that the density in the interfacial region be assumed to be a constant.

#### 4.2. A discontinuous thin film

The most important point to reemphasize is that Section 4 applies to the discontinuous film shown in Fig. 3.

Section 4.1 also applies to discontinuous films, with the understanding that the interfacial tensions or energies are those attributable to dividing surfaces separating semi-infinite regions; they are independent of position, in the absence of temperature or concentration gradients. These are the interfacial tensions or energies that are commonly used in the literature. The “true” interfacial tensions would be functions of distance to the common line.

### 5. One thin lens or fracture

Returning to view (c) of the interfacial region, consider the thin lens or fracture shown in Fig. 5, but no excess properties are associated with the dividing surface.

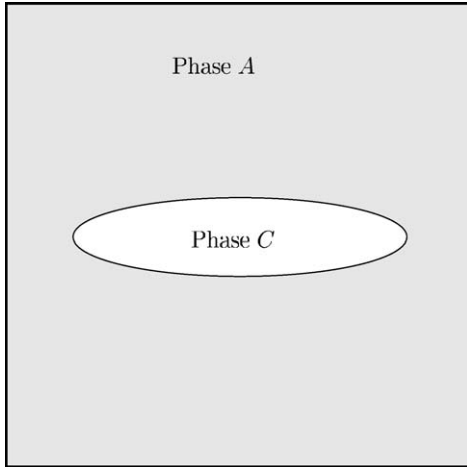


Fig. 5. A thin lens (or fracture) of phase C in phase A.

As suggested in the assumptions above, the net correction for intermolecular forces at each point in phase A is

$$\begin{aligned} \mathbf{b}^{(A,\text{corr})} &\equiv - \int_{R^{(C)}} \mathbf{f}^{(A,A)} \, d\mathbf{r} + \int_{R^{(C)}} \mathbf{f}^{(A,C)} \, d\mathbf{r} \\ &= \nabla \int_{R^{(C)}} n^{(A)2} \phi^{(A,A)} \, d\mathbf{r} \\ &\quad - \nabla \int_{R^{(C)}} n^{(A)} n^{(C)} \phi^{(A,C)} \, d\mathbf{r} \\ &= -\nabla \Phi^{(A,\text{corr})}, \end{aligned} \tag{51}$$

where

$$\begin{aligned} \Phi^{(A,\text{corr})} &\equiv - \int_{R^{(C)}} n^{(A)2} \phi^{(A,A)} \, d\mathbf{r} \\ &\quad + \int_{R^{(C)}} n^{(A)} n^{(C)} \phi^{(A,C)} \, d\mathbf{r}. \end{aligned} \tag{52}$$

In a similar way, we conclude that

$$\begin{aligned} \mathbf{b}^{(C,\text{corr})} &\equiv - \int_{R^{(A)}} \mathbf{f}^{(C,C)} \, d\mathbf{r} + \int_{R^{(A)}} \mathbf{f}^{(A,C)} \, d\mathbf{r} \\ &= \nabla \int_{R^{(A)}} n^{(C)2} \phi^{(C,C)} \, d\mathbf{r} \\ &\quad - \nabla \int_{R^{(A)}} n^{(A)} n^{(C)} \phi^{(A,C)} \, d\mathbf{r} \\ &= -\nabla \Phi^{(C,\text{corr})}. \end{aligned} \tag{53}$$

Here

$$\begin{aligned} \Phi^{(C,\text{corr})} &\equiv - \int_{R^{(A)}} n^{(C)2} \phi^{(C,C)} \, d\mathbf{r} \\ &\quad + \int_{R^{(A)}} n^{(A)} n^{(C)} \phi^{(A,C)} \, d\mathbf{r}. \end{aligned} \tag{54}$$

5.1. One thin lens or fracture, phase C is a vacuum

Let us assume that phase C is a vacuum, but let us now adopt view (b) of the interfacial region, in which bulk descriptions of material behavior is used, and interfacial energies or tensions is introduced in the dividing surface.

If in Section 5 phase C is a vacuum, those results become

$$\begin{aligned} \mathbf{b}^{(A)} &\equiv - \int_{R^{(C)}} \mathbf{f}^{(A,A)} \, d\mathbf{r} \\ &= \nabla \int_{R^{(C)}} n^{(A)2} \phi^{(A,A)} \, d\mathbf{r} \\ &= -\nabla \Phi^{(A,\text{corr})}, \end{aligned} \tag{55}$$

where

$$\Phi^{(A,\text{corr})} \equiv - \int_{R^{(C)}} n^{(A)2} \phi^{(A,A)} \, d\mathbf{r}. \tag{56}$$

5.2. One thin lens or fracture, phase C is a vacuum: with interfacial energy or tension

The introduction of interfacial energy or tension in Section 3.1 can be immediately extended to this case to conclude that

$$\mathbf{b}^{(C,\text{corr})\infty} = 0. \tag{57}$$

It is important to realize that, in contrast with Section 3.1, Eq. (20) in this context requires

$$\gamma \equiv \int_0^{\lambda^+} \Phi^{(A,\text{corr})} \, d\lambda. \tag{58}$$

Since  $\Phi^{(A,\text{corr})}$  is a function of lateral position with respect to the lens as well as distance from the lens,  $\gamma$  will be a function of position on the surface of the lens. Since the configuration of the lens or fracture will in general not be known and the computation of  $\Phi^{(A,\text{corr})}$  and  $\gamma$  require the configuration of the lens, this would result in an awkward computation. It is for this reason that we recommend that view (b) of the interfacial region and surface tension not be used in analyzing these problems.

6. Application on static contact angle

Contact angle measurement has various application in science and technology. Yet theoretical prediction of contact angle is still unclear. Young’s Equation (Young, 1805) interrelates the contact angle and surface tensions of the liquid and solid phases which has been used for almost 200 years. In this section, we will consider the intermolecular forces into the study and also propose a different approach than the traditional way of using Young’s equation.

It has been recognized for a long time that the molecular interactions play an important role within the immediate neighborhood of a three-phase common line where the meniscal film is very thin. The knowledge of bulk properties of liquid and solid is not enough for the theoretical prediction. The configuration of the fluid–fluid interface in the common line region and static contact angle depend on the correction for intermolecular forces.

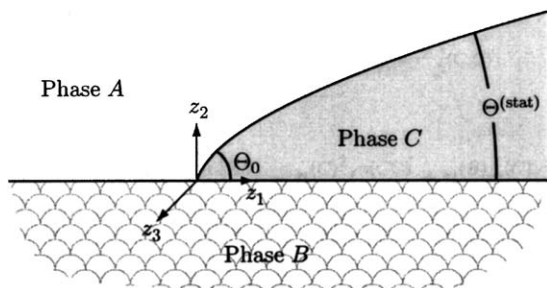


Fig. 6. A thin discontinuous film C forms a common line.

Rayleigh (1890) recognized that, in two dimensions sufficiently far away from the common line, the fluid–fluid interface approaches a plane inclined at a angle  $\Theta^{(\text{stat})}$  to the solid surface. As the common line is approached, the curvature of the interface is determined by a force balance to form a different angle  $\Theta_0$  with the solid surface. More recently, the configuration of the interface near the common line has been investigated in the context of statistical mechanics (Berry, 1974; Benner Jr. et al. 1982) and by molecular dynamics simulations (Saville, 1978). See Dussan V (1979) for a further review.

Fox and Zisman (1950) did a series of experiment on contact angles and liquid–liquid surface tension which is considered one of the most successful experimental work in this field. Also, contact angle problem has been discussed theoretically by many investigators (Dzyaloshinskii et al., 1960; Padday and Uffindell, 1968; Israelachvili, 1973; Miller and Ruckenstein, 1974; Jameson and del Cerro, 1976; Martynov et al., 1977; Hough and White, 1980; Wayner, 1980, 1982; Joanny and deGennes, 1984, 1986).

Fig. 6 shows in two dimensions the three-phase common line formed at equilibrium between phases A, C, and a solid B. The static contact angle  $\Theta^{(\text{stat})}$  might be measured by an experimentalist at some distance from the common line, using perhaps  $10\times$  magnification. Hough and White (1980) calculated Hamaker constants from Lifshitz theory and applied them to describe contact angles of alkanes on polytetrafluoroethylene (PTFE). They did well for predicting contact angles of large alkane carbon number but failed for small alkane carbon number comparing with Zisman's experimental data. In this section, we predict contact angles for all alkanes on PTFE very well and have good agreements with experimental values of contact angles for other dispersive liquids on PDMS.

### 6.1. Problem statement

The objective is to determine the experimentally measured static contact angle  $\Theta^{(\text{stat})}$ , which we will distinguish from  $\Theta_0$  shown in Fig. 6, the contact angle at the true common line. We will focus on the thin (precursor) film (Slattery, 1990, Section 1.2.9) formed in the neighborhood of the true common line.

Three assumptions are made.

- (i) The solid is rigid, and its surface is smooth and planar. Because the effect of gravity will be ignored with respect to the correction for intermolecular forces, its orientation with respect to gravity is arbitrary.
- (ii) The system is static, and equilibrium has been established. There are no interfacial tension gradients developed in the system.
- (iii) The correction for intermolecular forces will be introduced as described in Section 4.1.

In constructing this analysis, there are two important steps. First, how to compute intermolecular force correction term; second, how might the correction term be taken into account in the context of continuum mechanics for this problem.

### 6.2. Correction for long-range intermolecular forces

From Fig. 6, this problem is visualized as one thin film with interfacial tension in both interfaces. We will adopt view (d) from Section 2, because each phase of the thin film is subjected to long-range intermolecular forces from the other two. As discussed in Section 4.1, we argue that the interfacial tension  $\gamma^{(AC)}$  and  $\gamma^{(BC)}$  cannot fully account for the correction that must be made to the intermolecular forces. There is an additional correction to be made.

From Eqs. (45) and (41), we have

$$\Phi^{(C,\text{corr})\infty} \equiv 0 \quad (59)$$

$$\begin{aligned} \Phi^{(A,\text{corr})\infty} & \equiv - \int_{R^{(B)}} \left[ n^{(A)} n^{(C)} \phi^{(A,C)} - n^{(A)} n^{(B)} \phi^{(A,B)} \right. \\ & \quad \left. - n^{(C)^2} \phi^{(C,C)} + n^{(B)} n^{(C)} \phi^{(B,C)} \right] \mathbf{dr} \\ & = \left[ n^{(A)} n^{(C)} C^{(AC)} - n^{(A)} n^{(B)} C^{(AB)} - n^{(C)^2} C^{(CC)} \right. \\ & \quad \left. + n^{(B)} n^{(C)} C^{(BC)} \right] \\ & \quad \times \int_{-\infty}^{\infty} \int_{-\infty}^0 \int_{-\infty}^{\infty} \left[ \sqrt{(z_1 - x)^2 + (z_2 - y)^2 + z^2} \right]^{-6} \\ & \quad \times dx dy dz \\ & = \frac{\pi}{6z_2^3} \left[ n^{(A)} n^{(C)} C^{(AC)} - n^{(A)} n^{(B)} C^{(AB)} - n^{(C)^2} C^{(CC)} \right. \\ & \quad \left. + n^{(B)} n^{(C)} C^{(BC)} \right]. \end{aligned} \quad (60)$$

Superscript  $(ACB)$  represents for species A and B interacting across an intermediate phase C. The London dispersion force coefficient C is related to the Hamaker constant A by Israelachvili (1991, p. 176)

$$A^{(AC)} = \pi^2 C^{(AC)} n^{(A)} n^{(C)}, \quad (61)$$

so that

$$\Phi^{(A,\text{corr})\infty} = \frac{1}{6\pi z_2^3} \left[ A^{(AC)} - A^{(ACB)} - A^{(CC)} + A^{(BC)} \right]. \quad (62)$$

### 6.3. Solving procedure

Referring to Fig. 6 and Slattery (1990, Table 2.4.2–6), the configuration of the A–C interface is unknown

$$z_2 = h(z_1) \quad (63)$$

assuming that the C–B interface is

$$z_2 = 0. \quad (64)$$

Both the  $z_1$  and  $z_2$  components of the jump momentum balance for the A–C interface reduces to

$$\text{at } z_2 = h: p^{(A)} - p^{(C)} = \gamma \frac{d^2 h}{dz_1^2} \left[ 1 + \left( \frac{dh}{dz_1} \right)^2 \right]^{-3/2}. \quad (65)$$

Here  $p^{(A)}$  and  $p^{(C)}$  are the pressures in these phases evaluated at the A–C interface. To simplify the equation, we use  $\gamma$ , instead of  $\gamma^{(AC)}$ , as the surface tension between A and C. The static differential momentum balances are from Eq. (9)

$$\begin{aligned} \mathcal{P}^{(A)} &\equiv p^{(A)} + \Phi^{(A,\text{corr})\infty} \\ &= C_1 \end{aligned} \quad (66)$$

and

$$\begin{aligned} \mathcal{P}^{(C)} &\equiv p^{(C)} + \Phi^{(C,\text{corr})\infty} \\ &= C_2 \end{aligned} \quad (67)$$

in which  $C_1$  and  $C_2$  are constants. This permits us to write Eq. (65) as

$$\begin{aligned} C_1 - C_2 + \Phi^{(C,\text{corr})\infty} - \Phi^{(A,\text{corr})\infty} \\ = \gamma \frac{d^2 h}{dz_1^2} \left[ 1 + \left( \frac{dh}{dz_1} \right)^2 \right]^{-3/2} \end{aligned} \quad (68)$$

or, in view of Eqs. (59) and (60)

$$\begin{aligned} C_1 - C_2 + \frac{A^{(ACB)} - A^{(AC)} + A^{(CC)} - A^{(BC)}}{6\pi h^3} \\ = \gamma \frac{d^2 h}{dz_1^2} \left[ 1 + \left( \frac{dh}{dz_1} \right)^2 \right]^{-3/2}. \end{aligned} \quad (69)$$

Let us introduce as dimensionless variables

$$\begin{aligned} h^* &\equiv \frac{h}{\delta^{(BC)}}, \quad z_1^* \equiv \frac{z_1}{\delta^{(BC)}} \\ B^* &\equiv \frac{A^{(ACB)} - A^{(AC)} + A^{(CC)} - A^{(BC)}}{6\pi\gamma\delta^{(BC)2}}, \\ C_i^* &\equiv \frac{C_i\delta^{(BC)}}{\gamma}, \end{aligned} \quad (70)$$

where  $\delta^{(BC)}$  is the interface separation distance between phases B and C. We will explain how to get its value in Section 6.4. This permits us to express Eq. (69) as

$$C_1^* - C_2^* + \frac{B^*}{h^{*3}} = \frac{d^2 h^*}{dz_1^{*2}} \left[ 1 + \left( \frac{dh^*}{dz_1^*} \right)^2 \right]^{-3/2}. \quad (71)$$

The quantity  $C_1 - C_2$  represents the pressure difference across the interface as  $z_1 \rightarrow \infty$ . We can safely estimate that

$$|C_1^* - C_2^*| \ll |B^*| \quad (72)$$

in which case Eq. (71) reduces to

$$\frac{B^*}{h^{*3}} = \frac{d^2 h^*}{dz_1^{*2}} \left[ 1 + \left( \frac{dh^*}{dz_1^*} \right)^2 \right]^{-3/2}. \quad (73)$$

Our objective is to solve Eq. (73) consistent with the following conditions:

$$\text{at } z_1^* = 0: h^* = 1 \quad (74)$$

$$\text{at } z_1^* = 0: \frac{dh^*}{dz_1^*} = \tan \Theta_0, \quad (75)$$

where  $\Theta_0$  is the contact angle at the true common line.

Noting that

$$\begin{aligned} \frac{d^2 h^*}{dz_1^{*2}} &= \frac{dh^*}{dz_1^*} \frac{d^2 h^*}{dz_1^{*2}} \frac{dz_1^*}{dh^*} \\ &= \frac{1}{2} \frac{d}{dz_1^*} \left( \frac{dh^*}{dz_1^*} \right)^2 \frac{dz_1^*}{dh^*} \\ &= \frac{1}{2} \frac{d}{dh^*} \left( \frac{dh^*}{dz_1^*} \right)^2, \end{aligned} \quad (76)$$

we may write Eq. (73) as

$$\frac{B^*}{h^{*3}} = \frac{1}{2} \frac{d}{dh^*} \left( \frac{dh^*}{dz_1^*} \right)^2 \left[ 1 + \left( \frac{dh^*}{dz_1^*} \right)^2 \right]^{-3/2}. \quad (77)$$

Integrating this once consistent with Eqs. (74) and (75), we have

$$\begin{aligned} (1 + \tan^2 \Theta_0)^{-1/2} - \left[ 1 + \left( \frac{dh^*}{dz_1^*} \right)^2 \right]^{-1/2} \\ = -\frac{B^*}{2} \left( \frac{1}{h^{*2}} - 1 \right). \end{aligned} \quad (78)$$

In the limits

$$\text{as } z_1^* \rightarrow \infty: h^* \rightarrow \infty \quad (79)$$

and

$$\text{as } z_1^* \rightarrow 0: \frac{dh^*}{dz_1^*} \rightarrow \Theta^{(\text{stat})} \quad (80)$$

Eq. (78) further reduces to

$$(1 + \tan^2 \Theta_0)^{-1/2} - (1 + \tan^2 \Theta^{(\text{stat})})^{-1/2} = \frac{B^*}{2} \quad (81)$$

or

$$|\cos \Theta_0| - |\cos \Theta^{(\text{stat})}| = \mp \frac{A^{(ACB)} - A^{(AC)} + A^{(CC)} - A^{(BC)}}{12\pi\gamma\delta^{(BC)2}}. \quad (82)$$

For the case in which phase  $A$  is a gas, this reduces in view of that Hamaker constants  $A^{(AC)}$  and  $A^{(AB)}$ , which involve gas, are negligible to  $A^{(CC)}$  and  $A^{(BC)}$ :

$$|\cos \Theta_0| - |\cos \Theta^{(\text{stat})}| = \mp \frac{A^{(CC)} - A^{(BC)}}{12\pi\gamma\delta^{(BC)2}}. \quad (83)$$

The angle  $\Theta_0$  at the true common line should be determined using Young's equation (Slattery, 1990, p. 169):

$$\gamma^{(AC)} \cos \Theta_0 = \gamma^{(AB)} - \gamma^{(BC)}. \quad (84)$$

After some arrangement, we rewrite Eq. (83) as

$$\cos \Theta^{(\text{stat})} = \frac{\gamma^{(AB)} - \gamma^{(BC)}}{\gamma^{(AC)}} + \frac{A^{(CC)} - A^{(BC)}}{12\pi\gamma^{(AC)}\delta^{(BC)2}}. \quad (85)$$

#### 6.4. Prediction of $\Theta^{(\text{stat})}$

We will validate Eq. (85) by predicting  $\Theta^{(\text{stat})}$  for the  $n$ -alkanes against air on (PTFE) and various dispersive liquids against air on Polydimethylsiloxane(PDMS).

The Hamaker constants  $A^{(BC)}$  and  $A^{(CC)}$  were calculated by Hough and White (1980), and  $\gamma^{(AC)}$  were measured by Fox and Zisman (1950).

Girifalco and Good (1957) (see also Adamson, 1976, p. 360) proposed that  $\gamma^{(BC)}$  could be estimated as

$$\gamma^{(BC)} = \left( \sqrt{\gamma^{(AC)}} - \sqrt{\gamma^{(AB)}} \right)^2 = \gamma^{AB} + \gamma^{AC} - 2(\gamma^{AB}\gamma^{AC})^{1/2}. \quad (86)$$

It is important to recognize that the  $n$ -alkanes are volatile liquids and that the gas phase is dependent upon the specific  $n$ -alkane being considered. Fox and Zisman (1950) observed that there is no difference between contact angles measured in saturated air and those measured in unsaturated air. The conclusion is that  $\gamma^{(AB)}$  is independent of the particular  $n$ -alkane being considered. From Eqs. (84) and (86), we conclude that

$$\gamma^{(AC)} \cos \Theta_0 = \gamma^{(AB)} - \left[ \gamma^{(AB)} + \gamma^{(AC)} - 2(\gamma^{(AB)}\gamma^{(AC)})^{1/2} \right] \quad (87)$$

or

$$\cos \Theta_0 = -1 + 2 \left( \frac{\gamma^{(AC)}}{\gamma^{(AB)}} \right)^{1/2}. \quad (88)$$

As the alkane number  $n$  is decreased, there is a limiting value at which spontaneous wetting occurs, and  $\Theta_0 = \Theta^{(\text{stat})} = 0$

and  $\gamma^{(AB)} = \gamma^{(AC)}$ . In this way, Zisman (1962, p. 190) (see also Zisman, 1964, p. 20) concluded that

$$\gamma^{(AB)} = 18.5 \text{ mN/m}. \quad (89)$$

Working with different liquids on PTFE, Owens and Wendt (1969) came to the same conclusion.

In their analysis of supercritical adsorption of argon and krypton on impermeable carbon spheres, Fu et al. (2004) chose  $\delta$  as the position at which attractive and repulsive forces between the carbon and the gas, as described by a two-point Leonard–Jones potential, were balanced and  $\Phi^{(f,\text{corr})} = 0$ . Here we cannot do exactly the same thing, because our two-point potentials include only attractive forces. However, their approach inspires us to use a hard-sphere repulsion, estimating  $\delta^{(BC)}$  as the apparent radius of the repeating–CH<sub>2</sub>–groups in the  $n$ -alkanes immediately adjacent to the PTFE (planar) surface. In estimating the apparent radius of the–CH<sub>2</sub>–groups, we will assume that they are spheres in hexagonal close packing on the PTFE plane:

$$\delta^{(BC)} = 1.062[M^{(C)} / (\rho^{(C)} n_u N)]^{1/3}. \quad (90)$$

Here  $M^{(C)}$  is the molecular weight of phase  $C$ ,  $\rho^{(C)}$  is the mass density of phase  $C$ ,  $n_u$  is the number of repeating units in the molecule, and  $N$  is Avogadro's number.

Table 2 compares our calculation with experimental data and a previous theory. We get excellent agreement for all the  $n$ -alkanes while Hough and White (1980) only did well for alkanes with large carbon number.

Table 3 shows the good results for another system:  $A$  is air,  $B$  is PDMS and  $C$  is one of the dispersive liquids. The calculated results are still from Eq. (85). The experimental data are from different sources (Chaudhury and Whitesides, 1991; Baier and Meyer, 1992; Bowers and Zisman, 1964).

#### 6.5. Young's equation

Commonly in the literature, Young's equation is written as

$$\gamma^{(AC)} \cos \Theta^{(\text{stat})} = \gamma^{(AB)} - \gamma^{(BC)} \quad (91)$$

and applied at the apparent common line (as seen with 10× magnification). Tables 2 and 3 demonstrate that Eq. (91) does not represent the experimental measurements of  $\Theta^{(\text{stat})}$  well.

Slattery (1990, p. 169) derives Young's equation as Eq. (84), and applies it at the true common line as we do here. Eq. (85), which was developed using Eq. (84), represents the experimental data in Tables 2 and 3 much better than does Eq. (91). Our conclusion is that Eq. (84) is the preferred form of Young's equation.

## 7. Summary

Continuum mechanics has been extended to the nanoscale (not the molecular scale). In the context of continuum mechanics, nanoscale problems always involve the immediate

Table 2

Comparison of calculation and experimental data of static contact angle  $\Theta^{(\text{stat})}$  for *n*-alkanes on PTFE

<i>n</i> -alkanes	$\gamma^{(AC)}$ (mN/m)	$\delta^{(BC)a}$ (Å)	$A^{(BC)b}$ ( $10^{-20}$ J)	$A^{(CC)b}$ ( $10^{-20}$ J)	$\Theta^{(\text{cal})c}$ (deg)	$\Theta^{(\text{cal})d}$ (deg)	$\Theta^{(\text{cal})e}$ (deg)	$\Theta^{(\text{exp})f}$ (deg)
Heptane	20.3	3.097	4.03	4.31	29.1	26.0	20.0	21.0
Octane	21.8	3.085	4.11	4.49	33.5	33.7	28.2	26.0
Nonane	22.9	3.073	4.18	4.66	36.9	38.0	32.3	32.0
Decane	23.9	3.067	4.25	4.81	39.8	41.4	35.5	35.0
Undecane	24.7	3.061	4.28	4.87	40.7	43.8	38.1	39.0
Dodecane	25.4	3.056	4.35	5.03	43.1	45.8	39.6	42.0
Tetradecane	26.7	3.050	4.38	5.09	44.1	49.0	43.3	44.0
Hexadecane	27.6	3.044	4.43	5.22	45.8	51.1	45.1	46.0

<sup>a</sup>Calculated by Eq. (90).<sup>b</sup>Provided by Hough and White (1980).<sup>c</sup>Calculated by Hough and White (1980).<sup>d</sup>Calculated using Young's equation (84), replacing  $\Theta_0$  by  $\Theta^{(\text{stat})}$  as in the common use of Young's equation.<sup>e</sup>Calculated by Eq. (85).<sup>f</sup>Measured by Fox and Zisman (1950).

Table 3

Comparison of calculation and experimental data of static contact angle  $\Theta^{(\text{stat})}$  for dispersive liquids on PDMS

Liquids	$\gamma^{(AC)}$ (mN/m)	$\delta^{(BC)a}$ Å	$A^{(BC)b}$ $10^{-20}$ J	$A^{(CC)b}$ $10^{-20}$ J	$\Theta^{(\text{cal})c}$ (deg)	$\Theta^{(\text{cal})d}$ (deg)	$\Theta^{(\text{exp})e}$ (deg)
Diiodomethane	50.8	3.178	5.57	7.18	71.9	66.8	70.0 <sup>e</sup>
Bromonaphthalene	44.4	2.497	5.05	5.93	66.4	61.0	62.0 <sup>f</sup>
Methylnaphthalene	39.8	2.378	4.80	5.35	61.3	50.5	52.0 <sup>f</sup>
<i>Tert</i> -butyl naphthalene	33.7	3.384	4.76	5.23	52.5	50.1	49.0 <sup>g</sup>
Liq. paraffin	32.4	3.139	5.15	6.03	50.2	44.5	40.0 <sup>e</sup>
Hexadecane	27.6	3.044	4.80	5.22	38.6	34.4	36.0 <sup>g</sup>

<sup>a</sup>Calculated by Eq. (90).<sup>b</sup>Provided by Drummond and Chan (1997).<sup>c</sup>Calculated using Young's equation (84), replacing  $\Theta_0$  by  $\Theta^{(\text{stat})}$  as in the common use of Young's equation.<sup>d</sup>Calculated by Eq. (85).<sup>e</sup>Measured by Chaudhury and Whitesides (1991).<sup>f</sup>Measured by Baier and Meyer (1992).<sup>g</sup>Measured by Bowers and Zisman (1964).

neighborhood of a phase interface or the immediate neighborhood of a three-phase line of contact or common line. Although the presentation is new, it is based upon a long history of important developments beginning at least with that of Hamaker (1937).

This extension of continuum mechanics has been tested in the context of three applications.

- (1) A variety of static contact angles  $\Theta^{(\text{stat})}$  have been predicted with no adjustable parameters. At least for the systems studied and the experimental data reported, Eq. (85) is superior to previous theories.
- (2) The prediction for the surface tension of the *n*-alkanes requires one adjustable parameter. It is slightly better than the result of Israelachvili (1991, pp. 202, 203, 313), which also requires one adjustable parameter in describing the separation distance.
- (3) Fu et al. (2004) analyzed the supercritical adsorption of argon, krypton, and methane on impermeable carbon spheres. Their comparisons with previously reported experimental observations are significantly better than the results of previously reported alternative theories.

Beyond the comparisons with experimental data, our contact angle analysis provides us with a successful test of the form of Young's equation (84) derived by Slattery (1990, p. 169) for the true common line. As originally intended, Young's equation is applied at the apparent common line with  $\Theta_0$  (as observed at the true common line) replaced by  $\Theta^{(\text{stat})}$  (as observed at the apparent common line as seen by an experimentalist with, say,  $10\times$  magnification).

## Notation

### Roman symbols

$A^{(AB)}$	Hamaker constant between phases <i>A</i> and <i>B</i>
$A^{(ACB)}$	Hamaker constant for species <i>A</i> and <i>B</i> interacting across an interface phase <i>C</i>
<b>b</b>	body force per unit mass
$\mathbf{b}^{(A,\text{corr})}$	body force per unit volume at a point in phase <i>A</i> . This is introduced to correct for the use of bulk material behavior in the interfacial region

$\mathbf{b}^{(A,\text{corr})\infty}$	body force per unit volume at a point in phase A. This is introduced to correct for the use of surface tension on a dividing surface
$B^*$	dimensionless variable introduced in Eq. (70)
$C^{(AB)}$	London dispersion force coefficient between phases A and B
$\mathbf{f}^{(A,B)}$	force per unit volume of phase A per unit volume of phase B
$h$	configuration of the A–C interface
$M^C$	molecular weight of material C
$n^{(A)}$	number density at the specified point in phase A
$n_u$	number of repeating units in the molecule
$N$	Avogadro's number
$P$	thermodynamic pressure
$\mathcal{P}$	modified pressure defined in Eq. (47)
$\mathbf{P}$	projection tensor (Slattery, 1990, p. 1085)
$R^{(A)}$	region occupied by phase A
$\mathbf{S}$	extra stress defined in Eq. (46)
$\mathbf{T}$	bulk stress tensor using bulk description of material behavior
$\mathbf{T}^{(I)}$	stress tensor using real description of material behavior
$\mathbf{T}^{(I,\text{bulk})}$	stress tensor using bulk description of material behavior, corrected for intermolecular forces from the adjoining phase
$\mathbf{T}^{(\sigma)}$	surface stress tensor, stress tensor on a dividing surface
$\mathbf{v}^{(I)}$	velocity using real description of material behavior
$\mathbf{v}^{(I,\text{bulk})}$	velocity using bulk description of material behavior, corrected for intermolecular forces from the adjoining phase
$\mathbf{v}^{(\sigma)}$	surface velocity, velocity on a dividing surface
$z_i$	coordinates shown in Fig. 6

### Greek letters

$\gamma$	surface tension (or energy)
$\gamma^{(AC)}$	surface tension between phases A and C
$\delta^{(AB)}$	separation distance between phases A and B
$\Theta_0$	contact angle at the true common line
$\Theta^{(\text{stat})}$	static contact angle at the apparent common line
$\varepsilon^{(A,B)}$	well depth for two molecules A and B
$\lambda$	distance measured along the normal to the dividing surface
$\boldsymbol{\xi}^{(\alpha)}$	unit normal to the interface pointing into phase $\alpha$
$\rho^{(I)}$	bulk density using real description of material behavior
$\rho^{(I,\text{bulk})}$	bulk density using bulk description of material behavior, corrected for intermolecular forces from the adjoining phase
$\rho^{(\sigma)}$	surface density, density on a dividing surface
$\sigma^{(A,B)}$	collision diameter for two molecules A and B
$\phi^{(AC)}$	potential energy for two molecules A and C separated by a distance

$\Phi^{(A,\text{corr})}$	net correction for intermolecular potential at a point in phase A
$\Phi^{(A,\text{corr})\infty}$	net correction for intermolecular potential at a point in phase A when the surface tension is introduced to the dividing surface

### References

- Adamson, A.W., 1976. *Physical Chemistry of Surfaces*. third ed. Wiley, New York.
- Baier, R.E., Meyer, A.E., 1992. Surface analysis of fouling-resistant marine coatings. *Biofouling* 6, 165–180.
- Benner Jr., R.E., Scriven, L.E., Davis, H.T., 1982. Structure and stress in the gas–liquid solid contact region. *Faraday Symposium, The Royal Society of Chemistry* 16, 169–190.
- Berry, M.V., 1974. Simple fluids near rigid solids—statistical-mechanics of density and contact angle. *Journal of Physics A: Mathematical and General* 7, 231–245.
- Bird, R.B., Stewart, W.E., Lightfoot, E.N., 2002. *Transport Phenomena*. second ed. Wiley, New York.
- Bowen, W.R., Jenner, F., 1995. The calculation of dispersion forces for engineering applications. *Advances in Colloid and Interface Science* 56, 201–243.
- Bowers, R.C., Zisman, W.A., 1964. Surface properties. In: Baer, E. (Ed.), *Engineering Design for Plastics*. Van Nostrand Reinhold Co., New York, pp. 689–741.
- Casimir, H., Polder, D., 1948. The influence of retardation on the London-van der Waals forces. *Physical Review* 73 (4), 360–372.
- Chaudhury, M.K., Whitesides, G.M., 1991. Direct measurement of interfacial interactions between semispherical lenses and flat sheets of polydimethylsiloxane and their chemical derivatives. *Langmuir* 7, 1013–1025.
- Drummond, C.J., Chan, D.Y.C., 1997. van der Waals interaction, surface free energies, and contact angles: dispersive polymers and liquids. *Langmuir* 13, 3890–3895.
- Dussan, V.E.B., 1979. Spreading of liquids on solid-surfaces—static and dynamic contact lines. *Annual Review of Fluid Mechanics* 11, 371–400.
- Dzyaloshinskii, I.E., Lifshitz, E.M., Pitaevskii, L.P., 1960. van der Waals forces in liquid films. *Soviet Physics JETP* 37, 161–170.
- Dzyaloshinskii, I.E., Lifshitz, E.M., Pitaevskii, L.P., 1961. The general theory of van der Waals forces. *Advances in Physics* 10, 165–209.
- Fox, H.W., Zisman, W.A., 1950. The spreading of liquids on low energy surfaces. i. polytetrafluoroethylene. *Journal of Colloid Science* 5, 514–531.
- Fu, K., Robinson, R.L., Slattery, J.C., 2004. An analysis of supercritical adsorption in the context of continuum mechanics. *Chemical Engineering Science* 59, 801–808.
- Girifalco, L.A., Good, R.J., 1957. A theory for the estimation of surface and interfacial energies. I. derivation and application to interfacial tension. *Journal of Physical Chemistry* 61, 904–909.
- Hamaker, H.C., 1937. The London-van der Waals attraction between spherical particles. *Physica* 4, 1058–1072.
- Hirschfelder, J.O., Curtiss, C., Bird, R.B., 1954. *Molecular Theory of Gases and Liquids*. Wiley, New York. corrected with notes added in 1964.
- Hough, D.B., White, L.R., 1980. The calculation of Hamaker constants from Lifshitz theory with applications to wetting phenomena. *Advances in Colloid and Interface Science* 14, 3–41.
- Israelachvili, J.N., 1973. van der Waals dispersion force contribution to works of adhesion and contact angles on basis of macroscopic theory. *Journal of Chemical Society of Faraday Transactions II* 69, 1729–1738.
- Israelachvili, J.N., 1991. *Intermolecular and Surface Forces*. second ed. Academic Press, London.

- Jameson, G.J., del Cerro, M.C.G., 1976. Theory for equilibrium contact-angle between a gas, a liquid and a solid. *Journal of the Chemical Faraday Transactions* 72, 883–895.
- Jasper, J.J., Kring, E.V., 1955. Thermodynamic properties of surfaces of a *n*-alkane series. *Journal of Physical Chemistry* 59, 1019–1021.
- Joanny, J.F., deGennes, P.G., 1984. A model for contact-angle hysteresis. *Journal of Chemical Physics* 81, 552–562.
- Joanny, J.F., deGennes, P.G., 1986. Role of long-range forces in heterogeneous nucleation. *Journal of Colloid and Interface Science* 111, 94–101.
- Lifshitz, E.M., 1956. The theory of molecular attraction forces between solid bodies. *Soviet Physics JETP* 2, 73–83.
- Mahanty, J., Ninham, B.W., 1976. *Dispersion Forces*. Academic Press, New York.
- Martynov, G.A., Starov, V.M., Churaev, N.V., 1977. Hysteresis of contact-angle at homogeneous surfaces. *Colloid Journal USSR* 39, 406–417.
- Miller, C.A., Ruckenstein, E., 1974. Origin of flow during wetting of solids. *Journal of Colloid and Interface Science* 48, 368–373.
- Owens, D.K., Wendt, R.C., 1969. Estimation of the surface free energy of polymers. *Journal of Applied Polymer Science* 13, 1741–1747.
- Padday, J.F., Uffindell, N.D., 1968. Calculation of cohesive and adhesive energies from intermolecular forces at a surface. *Journal of Physical Chemistry* 72, 1407–1414.
- Rayleigh, L., 1890. On the theory of surface forces. *Philosophical Magazine* 30, 285–298.
- Russel, W.B., Saville, D.A., Schowalter, W.R., 1989. *Colloidal Dispersions*. Cambridge University Press, Cambridge.
- Saville, G., 1978. Computer simulation of liquid–solid–vapor contact-angle. *Journal of the Chemical Society of Faraday Transactions* 73, 1122–1132.
- Slattery, J.C., 1990. *Interfacial Transport Phenomena*. Springer, New York.
- Slattery, J.C., 1999. *Advanced Transport Phenomena*. Cambridge University Press, New York.
- Steele, W.A., 1973. The physical interaction of gases with crystalline solids. *Surface Science* 36, 317–352.
- Steele, W.A., 1974. *The Interaction of Gases with Solid Surfaces*. Pergamon Press, New York.
- Steele, W.A., 1978. The interaction of rare gas atoms with graphitized carbon black. *Journal of Physical Chemistry* 82, 817–821.
- Truesdell, C., Toupin, R.A., 1960. The classical field theories. in: Flügge, S. (Ed.), *Handbuch der Physik*, vol. 3/1. Springer, Berlin, p. 226.
- Wayner, P.C., 1980. Interfacial profile in the contact line region of a finite contact-angle system. *Journal of Colloid and Interface Science* 77, 495–500.
- Wayner, P.C., 1982. The interfacial profile in the contact line region and Young-Dupre equation. *Journal of Colloid and Interface Science* 88, 294–295.
- Young, T., 1805. An essay on the cohesion of fluids. *Philosophical Transactions of the Royal Society of London* 95, 65–87.
- Zisman, W.A., 1962. Constitutional effects on adhesion and abhesion. In: Weiss, P. (Ed.), *Adhesion and Cohesion: Proceedings of the Symposium on Adhesion and Cohesion*. Elsevier, Amsterdam, pp. 176–208.
- Zisman, W.A., 1964. Contact angle, wettability, and adhesion. In: *Advances in Chemistry Services*, vol. 43. American Chemical Society, Washington, DC.